

DaTaSeg: Taming a Universal Multi-Dataset Multi-Task Segmentation Model

Xiuye Gu Yin Cui* Jonathan Huang* Abdullah Rashwan* Xuan Yang*
 Xingyi Zhou* Golnaz Ghiasi Weicheng Kuo Huizhong Chen Liang-Chieh Chen†

David Ross
 Google Research

Abstract

Observing the close relationship among panoptic, semantic and instance segmentation tasks, we propose to train a universal multi-dataset multi-task segmentation model: DaTaSeg. We use a shared representation (mask proposals with class predictions) for all tasks. To tackle task discrepancy, we adopt different merge operations and post-processing for different tasks. We also leverage weak-supervision, allowing our segmentation model to benefit from cheaper bounding box annotations. To share knowledge across datasets, we use text embeddings from the same semantic embedding space as classifiers and share all network parameters among datasets. We train DaTaSeg on ADE semantic, COCO panoptic, and Objects365 detection datasets. DaTaSeg improves performance on *all* datasets, especially small-scale datasets, achieving 54.0 mIoU on ADE semantic and 53.5 PQ on COCO panoptic. DaTaSeg also enables weakly-supervised knowledge transfer on ADE panoptic and Objects365 instance segmentation. Experiments show DaTaSeg scales with the number of training datasets and enables open-vocabulary segmentation through direct transfer. In addition, we annotate an Objects365 instance segmentation set of 1,000 images and will release it as a public benchmark.

1 Introduction

Image segmentation is a core computer vision task with wide applications in photo editing, medical imaging, autonomous driving, and beyond. To suit different needs, various forms of segmentation tasks have arisen, the most popular ones being panoptic [28], semantic [22], and instance [18] segmentation. Prior works generally use specific model architectures tailored to each individual task [27, 40, 5, 20]. However, these segmentation tasks are closely related, as they can all be regarded as grouping pixels and assigning a semantic label to each group [58]. In this paper, we address the following question: *Can we leverage a diverse collection of segmentation datasets to co-train a single model for all segmentation tasks?* A successful solution to this problem would leverage knowledge transfer among datasets, boosting model performance across the board especially on smaller datasets.

Existing works on unified segmentation models either focus on a single architecture to handle multiple tasks [9, 7, 67, 24], but with separate weights for different datasets; or a single set of weights for multiple datasets [26, 31, 70], but on the same task. By contrast, in this work, we aim to train a *single* model on *multiple* datasets for *multiple* tasks. Our key idea of unifying these segmentation tasks is to

*Equal contribution. Correspondence to: Xiuye Gu (xiuyegu@google.com).

†Work done while at Google. Now at ByteDance

use a universal intermediate mask representation: a set of mask proposals (*i.e.*, grouped pixels) with class labels [58, 9]. Different segmentation tasks can be realized by applying different merge and post-processing operations on this unified representation. This allows us to train our network on the same output space for different tasks. Furthermore, using this representation, we can exploit weak bounding box supervision for segmentation, which are far cheaper to collect than mask annotations.

To encourage knowledge sharing and transfer among the multiple segmentation sources, our network architecture shares the same set of weights across all datasets and tasks. In addition, we utilize text embeddings as the class classifier, which map class labels from different datasets into a *shared* semantic embedding space. This design further enhances knowledge sharing among categories with similar meanings in different datasets, *e.g.*, ‘windowpane’ and ‘window-other’. Our approach can be contrasted with an alternative of using dataset-specific model components — we show in our experiments that our simpler, unified approach leads to improved performance and enables open-vocabulary segmentation via simply switching the text embedding classifier.

Putting these techniques together, we propose **DaTaSeg**, a universal segmentation model, together with a cotraining recipe for the multi-task and multi-dataset setting. We train DaTaSeg on the ADE20k semantic [68], COCO panoptic [28], and Objects365 detection [51] datasets. We show that DaTaSeg improves performance on all datasets comparing with training separately, and significantly benefits relatively small-scale datasets (ADE20k semantic), outperforming a model trained only on ADE20k semantic by **+6.1** and **+5.1** mIoU with ResNet50 [21] and ViTDet-B [34] backbones. The multi-dataset multi-task setting also allows us to *seamlessly* perform weakly-supervised segmentation by transferring knowledge from other fully supervised source datasets, which we demonstrate on ADE20k panoptic and Objects365 instance segmentation. DaTaSeg also directly transfers to other datasets not seen during training. It outperforms open-vocabulary panoptic methods on Cityscapes panoptic dataset [10] and performs comparably with open-vocabulary segmentation works on Pascal Context semantic dataset [44].

To summarize our contributions, we present DaTaSeg, a single unified framework for multi-dataset multi-task segmentation. DaTaSeg leverages knowledge from multiple sources to boost performance on all datasets. It seamlessly enables weakly-supervised segmentation, directly transfers to other datasets and is capable of open-vocabulary segmentation. As an additional contribution, we have annotated a subset of the Objects365 validation set with groundtruth instance masks and will release them as an evaluation benchmark for instance segmentation.

2 Related Work

Muti-dataset training: Training on multiple datasets has become popular for developing robust computer vision models [59, 71, 31, 42, 56, 62]. For object detection, Wang *et al.* [59] train an object detector on 11 datasets in different domains and show improved robustness. UniDet [71] trains a unified detector on 4 large-scale detection datasets with an automatic label merging algorithm. DetectionHub [42] employs text embeddings to accommodate different vocabularies from multiple datasets, and features dataset-specific designs. For segmentation, MSeg [31] manually merges the vocabularies of 7 semantic segmentation datasets, and trains a unified model on all of them; however, the manual efforts are expensive and hard to scale. LMSeg [70] dynamically aligns segment queries with category embeddings. UniSeg [26] explores the label relation and conflicts between multiple datasets in a learned way. Most of these works merge datasets using a unified vocabulary on a single task, while our work focuses on a more challenging problem: we merge datasets with different vocabularies *and* different tasks.

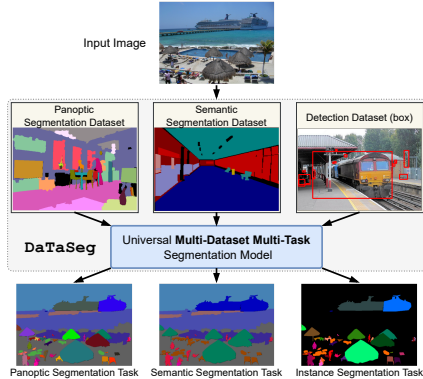


Figure 1: Considering the similarities across various segmentation tasks, and recognizing the potential for enhancing segmentation performance by harnessing data from multiple sources, **we propose to train a universal segmentation model, DaTaSeg, on multiple datasets to perform multiple segmentation tasks.**

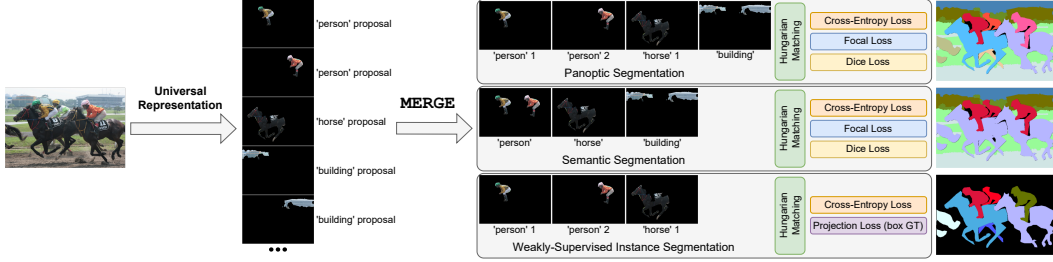


Figure 2: **Universal representation, MERGE operations, and losses for different segmentation tasks.** We use a universal representation for all tasks: a set of mask proposals with class predictions. Then we adopt distinct MERGE operations based on the segmentation task. For panoptic segmentation, we merge proposals predicting the same “stuff” category. For semantic segmentation, both “thing” and “stuff” categories undergo merging. In instance segmentation, we do not perform MERGE and there are no “stuff” categories. During training, we use Hungarian matching, and apply different losses based on the supervision types.

Unified segmentation model: Panoptic segmentation [28] unifies semantic and instance segmentation. Prior works [27, 61, 64, 6, 47] exploit separate modules for semantic segmentation [40, 5] and instance segmentation [18, 20], followed by another fusion module. Recently, the mask transformer framework proposed by MaX-DeepLab [58] directly predicts class-labeled masks, allowing end-to-end panoptic segmentation. MaskFormer [9] and K-Net [67] adopt a single transformer-based model for different segmentation tasks. Mask2Former [7] improves upon MaskFormer by proposing masked attention, while kMaX-DeepLab [65] develops k-means cross-attention. OneFormer [24] extends Mask2Former with a multi-task train-once design. All these works still train separate weights on *different* datasets. By contrast, we aim at a single unified model that can perform well across all segmentation tasks and datasets.

Weakly-supervised segmentation: Facing the issue of expensive segmentation annotations, many works have proposed to learn segmentation masks from cheaper forms of supervision [45, 11, 37]. In particular, box-supervised approaches are most related to our work, including BoxInst [54] and Cut-and-Paste [49] for instance segmentation, Box2Seg [30] and BCM [53] for semantic segmentation, and DiscoBox [32] and SimpleDoesIt [25] for both semantic and instance segmentation. Despite the popularity of box-driven semantic and instance segmentation, fewer attempts have been made at weakly-supervised panoptic segmentation. Li *et al.* [33] employ a pretrained model to generate pseudo-ground-truth in advance, in addition to weak supervision from bounding boxes and image level labels. Shen *et al.* [52] add a handcrafted branch on top of semantic and instance segmentation models to generate panoptic proposals. Unlike these methods that require customized components, our approach can realize knowledge sharing among datasets with different forms of annotations in a more systematic and data-centric fashion, and seamlessly enable weakly-supervised segmentation.

3 Method

3.1 A universal segmentation representation

Segmentation aims to group pixels of the same concept together. We propose to use an intermediate and universal representation, namely mask proposals, for all segmentation tasks. A mask proposal is a binary foreground mask with a class prediction. We use this representation for its versatility: one mask proposal can represent a single instance, any number of instances, a region, or even a part of an object. They can overlap and can be combined to form higher-level segmentation outputs — an instance (thing) or a region of the same semantic class (stuff). Thus they are well suited for the different flavors of segmentation considered in this paper. We note that a similar concept has been used in existing works [58, 9, 7, 65], for specific segmentation tasks on a single dataset. We show this representation is especially beneficial in our multi-dataset setting, as different datasets define things and stuff differently. For example, ‘table’ is a thing category in the ADE20k panoptic dataset, but there is a ‘table-merged’ stuff category in COCO panoptic. In our framework, both thing and stuff categories are represented in this same representation, and we treat them differently in the next step.

3.2 Merging predictions for specific tasks

Notations: Let (\hat{z}_j, \hat{M}_j) denote the j -th mask proposal with its class prediction, where $\hat{M}_j \in \mathbb{R}^{H \times W}$ denotes (pre-sigmoid) logits for the mask proposal and $\hat{z}_{j,c_k} \in \mathbb{R}$ denotes the logit for class c_k . We assume a fixed set of N mask proposals. $\mathbb{C}_{d,thing}$ and $\mathbb{C}_{d,stuff}$ are the set of thing and stuff categories in dataset d .

Merge operation (MERGE): Given the varying formats of groundtruth annotations for different segmentation tasks, we propose a MERGE operation to merge the mask proposals predicting the same category c_k . We adopt a simple element-wise max operation to merge the mask proposal logits. In particular, the merged mask proposal logits at the (p, q) location for class c_k is computed as:

$$\mathcal{M}(c_k)_{p,q} = \max_j (\mathbb{1}[\arg\max(\hat{z}_j) = c_k] \cdot \hat{M}_{j,p,q}). \quad (1)$$

We choose element-wise max so that applying MERGE on raw mask logits is equivalent to applying MERGE on the soft mask predictions post-sigmoid. We also choose to merge at the level of raw logits for numerical stability. If no proposal predicts class c_k , then the corresponding merged mask $\mathcal{M}(c_k)_{p,q}$ is set to -100 to ensure it is close to 0 after sigmoid.

In addition to merging masks, we merge their corresponding class predictions by simply averaging the class prediction logits of the proposals predicting class c_k :

$$\mathcal{Z}(c_k) = \frac{\sum_j (\mathbb{1}[\arg\max(\hat{z}_j) = c_k] \cdot \hat{z}_j)}{\sum_j (\mathbb{1}[\arg\max(\hat{z}_j) = c_k]) + \epsilon}, \quad (2)$$

where ϵ is a small number to prevent division by zero.

How we apply the above merge operations depends on the task, as we now describe:

Panoptic segmentation: To make the predicted mask proposals have the same format as the groundtruth, we apply MERGE to all stuff categories $c_k \in \mathbb{C}_{d,stuff}$.

Semantic segmentation: In contrast with panoptic segmentation, the semantic segmentation groundtruth for each thing category is also a single mask (*i.e.*, thing categories are treated equivalently as stuff categories). We thus apply MERGE to all predicted mask proposals to cover all thing and stuff categories $\mathbb{C}_{d,stuff} \cup \mathbb{C}_{d,thing}$.

Instance segmentation: MERGE is not needed in this task, since the desired outputs are separate masks for separate instances. There are no stuff categories in the vocabulary ($\mathbb{C}_{d,stuff} = \emptyset$), and therefore no stuff proposals.

Training: During training, we apply the corresponding MERGE operations based on the segmentation task. We then use one-to-one Hungarian matching [29] to match the merged outputs with the groundtruth, and calculate the training losses. Detailed training losses are provided in Sec. 3.5.

Inference: At inference time, we apply the same MERGE operations to predicted mask proposals based on the given task. We post-process the mask proposals to obtain non-overlapping outputs for panoptic and semantic segmentation. For instance segmentation, we simply take the top mask proposals as final outputs, since overlaps are allowed. Please refer to supplementary for more details.

We illustrate how the MERGE operation works for different segmentation tasks in Fig. 2.

3.3 Weakly-supervised instance segmentation

Bounding boxes are much cheaper to annotate than instance masks, and thus detection datasets can have a larger scale than instance segmentation datasets. In order to train on larger detection datasets with only bounding box annotations, as well as to demonstrate the versatility of our framework to handle various tasks, we propose to perform weak-bounding-box-supervised instance segmentation.

We adopt a simple projection loss \mathcal{L}_{proj} from [55], which measures consistency of vertical and horizontal projections of predicted masks \hat{M}_j against groundtruth boxes:

$$\mathcal{L}_{proj}(\hat{M}_j, b_j) = \mathcal{L}_{dice}(\text{Proj}_x(S(\hat{M}_j)), \text{Proj}_x(b_j)) + \mathcal{L}_{dice}(\text{Proj}_y(S(\hat{M}_j)), \text{Proj}_y(b_j)), \quad (3)$$

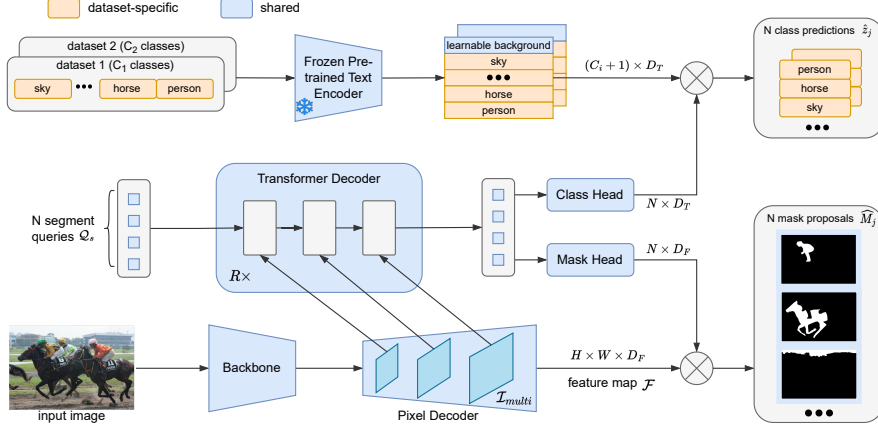


Figure 3: **Overview of our universal multi-dataset multi-task segmentation model (DaTaSeg).** We feed N learnable segment queries into a transformer decoder, which cross-attends to multi-scale image features from the pixel decoder. The outputs serve as the universal representation for all tasks: N mask proposals accompanied by N class predictions. To promote knowledge sharing, we **share** all network parameters across different datasets and tasks. The only **dataset-specific** design is a classifier consisting of frozen text embeddings of categories specific to each dataset. Additionally, we employ a **shared** learnable background classifier.

where \mathcal{L}_{dice} is the dice loss [43]; b_j is the groundtruth bounding box matched to j -th mask proposal prediction; $\text{Proj}_{x/y}$ denotes the projection operation along the x or y axis, which can be implemented by a max operation along the axis; and $S(\cdot)$ denotes the sigmoid function.

By itself, a box consistency loss such as Eqn. 3 is insufficient as a supervision signal for segmentation (e.g., Eqn. 3 is equally satisfied by predicting the bounding box of an object instead of its mask). Thus other works have resorted to additional, often more complex, loss terms (such as the pairwise affinity loss from [55]). However, by training on multiple datasets and multiple segmentation tasks, these handcrafted losses are not necessary, as our model can transfer knowledge from other fully-supervised tasks on other datasets.

3.4 Network architecture with knowledge sharing

Network architecture: We now describe the network architecture (similar to [7]) that predicts mask proposal and class prediction pairs (\hat{z}_j, \hat{M}_j) . The input image first goes through a *backbone*, and we use a *pixel decoder* to 1) output multi-scale image features \mathcal{I}_{multi} , and 2) output a high-resolution feature map \mathcal{F} that fuses information from the multi-scale image features. N mask proposal pairs are then generated from N learnable *segment queries* \mathcal{Q}_s : The segment queries are fed into a *transformer decoder*, which cross attends to multi-scale image features \mathcal{I}_{multi} from the pixel decoder. The N decoder outputs are then passed to class embedding and mask embedding heads (both MLPs) to obtain N (mask embedding, class embedding) pairs. To extract final mask proposals and class predictions, we apply a dot product between the high-resolution feature map \mathcal{F} and the mask embeddings to obtain N mask proposal logits \hat{M}_j . And to obtain class predictions, we compute dot products of the class embeddings against a per-category classifier w_k for each category c_k . Fig. 3 shows an overview.

Knowledge sharing: We bake knowledge sharing into our model in two ways. First, *all network parameters are shared* across all datasets, allowing knowledge sharing among different datasets and knowledge transfer among different tasks. Additionally, to share knowledge gathered from training samples of similar categories in multiple datasets, e.g., ‘windowpane’ in ADE20k and ‘window-other’ in COCO, we propose to *map all category names into a shared semantic embedding space*. We feed the category names into a frozen pre-trained text encoder to set the per-category classifier w_k . i.e., we let the fixed text embeddings serve as classifiers. This is similar to open-vocabulary segmentation [15], but with a different purpose: our focus here is on knowledge sharing among different datasets. This automatic approach scales better than manually unifying label spaces in different datasets [31].

3.5 Co-training strategy

We adopt a simple co-training strategy: at each iteration, we randomly sample *one* dataset, then sample an entire batch for that iteration from the selected dataset. This can be contrasted with sampling from multiple datasets at each iteration. The main advantage for our strategy is that it is simple to implement, and allows for more freedom to use different settings for different datasets, as well as to apply distinct losses to various tasks. To account for different dataset sizes, we use per-dataset sampling ratios, similar to [36].

For fully-supervised tasks, we employ direct *mask supervision*, which can be obtained from panoptic/semantic/instance segmentation groundtruth. To calculate the Hungarian matching cost and the training loss, we use a combination of focal binary cross-entropy loss \mathcal{L}_{focal} [39] and dice loss \mathcal{L}_{dice} [43], following [9]. Regarding *weak bounding box supervision*, we adopt the projection loss \mathcal{L}_{proj} introduced in Sec. 3.3 for the matching cost and training loss. In both cases of supervision, we use the negative of the class prediction probability p as the classification matching cost [4], and use cross-entropy loss \mathcal{L}_{ce} for training. The total training loss is:

$$\mathcal{L}_d = \lambda_{ce,d}\mathcal{L}_{ce} + \lambda_{focal,d}\mathcal{L}_{focal} + \lambda_{dice,d}\mathcal{L}_{dice} + \lambda_{proj,d}\mathcal{L}_{proj}. \quad (4)$$

The Hungarian matching cost is defined similarly:

$$\mathcal{C}_d = -\mu_{ce,d} \cdot p + \mu_{focal,d}\mathcal{L}_{focal} + \mu_{dice,d}\mathcal{L}_{dice} + \mu_{proj,d}\mathcal{L}_{proj}. \quad (5)$$

Here, $\lambda_{*,d}$ and $\mu_{*,d}$ are the weights for dataset d .

4 Experiments

Datasets and metrics: We train and evaluate DaTaSeg on COCO panoptic [28] and ADE20k semantic [68] using mask supervision, as well as Objects365-v2 [51] detection datasets using bounding box weak supervision. **COCO panoptic** is the most popular panoptic segmentation benchmark with 118,287 training images and 5,000 validation images. COCO has 80 thing categories and 53 stuff categories. **ADE20k semantic** is one of the most widely used semantic segmentation benchmarks with 150 categories, 20,210 training images, and 2,000 validation images.

For evaluation, besides the training datasets, we also evaluate on **ADE20k panoptic**, which uses the same validation images as ADE20k semantic but with panoptic annotations. The original 150 categories are divided into 100 thing categories and 50 stuff categories. Finally, we train on the **Objects365-v2 detection** (bounding boxes only) dataset, which has 365 categories and 1,662,292 training images. To evaluate the weakly-supervised instance segmentation results, we manually label a subset of 1,000 images from the Objects365 validation set. Our annotation pipeline involves 20 well-trained human annotators, following the protocol in [2], without using any automatic assistant tools. We will release this **Objects365 instance segmentation validation set** as a public benchmark.

To compare DaTaSeg with the state-of-the-art methods, we in addition evaluate on popular open-vocabulary segmentation benchmarks. Following OpenSeg [15], we evaluate on **PASCAL Context** datasets [44] with 5k val images. We use its two versions: 59 classes (**PC-59**) and 459 classes (**PC-459**). We also evaluate on the 500-image val set of **Cityscapes** panoptic dataset [10], which focuses on urban street scenes with 11 stuff categories and 8 thing categories.

We report results in standard evaluation metrics: panoptic quality (**PQ**), mean intersection-over-union (**mIoU**), and mean average precision (**AP**) for panoptic, semantic, and instance segmentation, respectively.

Implementation details: We experiment with ResNet [21] or ViTDet [34] backbones. For ResNet, we use an ImageNet-1K [50] pretrained checkpoint, with a backbone learning rate multiplier of 0.1 [4]; the pixel decoder consists of a transformer encoder [57] and a modified FPN [38] following [9], except that we use Layer Norm [1] and GeLU [23] activation for training stability. For ViTDet, we use the ImageNet-1K MAE pretrained checkpoint [19] with the layerwise lr decay [34]; the pixel decoder is the simple feature pyramid inside ViTDet, whose outputs are upsampled and added together to get the high resolution feature map \mathcal{F} . The mask embedding head is a 3-layer MLP. The class embedding head contains a linear layer followed by ReLU. We use CLIP-L/14 [48] as the pretrained text encoder. We use 100 segment queries \mathcal{Q}_s , unless otherwise stated. See supplementary for more details.

Backbone	Model	Fully-Supervised		Weakly-Supervised Transfer	
		ADE	COCO	ADE	O365
		semantic mIoU	panoptic PQ	semantic \rightarrow panoptic PQ	box \rightarrow instance mask AP
ResNet50	Separate	42.0	48.2	26.9	12.3
	DaTaSeg	48.1 (+6.1)	49.0 (+0.8)	29.8 (+2.9)	14.3 (+2.0)
ViTDet-B	Separate	46.3	51.9	27.5	14.7
	DaTaSeg	51.4 (+5.1)	52.8 (+0.9)	32.9 (+5.4)	16.1 (+1.4)
ViTDet-L	DaTaSeg	54.0	53.5	33.4	16.4

Table 1: **Comparing DaTaSeg and separate dataset-specific models.** We show results on both the training tasks (fully-supervised) and new tasks (weakly-supervised transfer). Our single DaTaSeg outperforms separately trained models on *all* datasets. They are trained under the same settings, so the performance gains come from knowledge in other datasets through our multi-dataset multi-task cotraining recipe. We observe: 1) DaTaSeg *significantly* improves tasks with limited data (ADE20k semantic); 2) DaTaSeg enables weakly-supervised knowledge transfer (ADE20k panoptic and O365 instance); 3) DaTaSeg scales well with backbones.

Training sets			Fully-Supervised		Weakly-Supervised Transfer	
ADE	COCO	O365	ADE	COCO	ADE	O365
semantic	panoptic	bbox	semantic mIoU	panoptic PQ	semantic \rightarrow panoptic PQ	box \rightarrow instance mask AP
✓			42.0	8.4	26.7	1.0
	✓		15.3	48.2	11.6	5.8
		✓	11.0	12.4	5.8	12.3
✓		✓	46.3 (+4.3)	14.0	26.4 (-0.3)	15.0 (+2.7)
	✓	✓	18.3	48.9 (+0.7)	12.3	15.2 (+2.9)
✓	✓		47.3 (+5.3)	49.0 (+0.8)	30.5 (+3.8)	5.6
✓	✓	✓	48.1 (+6.1)	49.0 (+0.8)	29.8 (+2.9)	14.3 (+2.0)

Table 2: **Importance of training on multiple datasets.** We train DaTaSeg on all combinations the three datasets. Experiments are done on ResNet50 under same settings. DaTaSeg scales with the number of training datasets.

4.1 DaTaSeg improves over dataset-specific models

As an apples-to-apples comparison, we separately train a model on each dataset. We ensure that the models see the same number of images in cotraining and separately-training for each dataset. Table 1 (left) shows the results. DaTaSeg outperforms separately trained models on all datasets. Since we use exactly the same settings, we attribute the performance boost to our multi-dataset multi-task training recipe, which harnesses knowledge from multiple sources. Especially, DaTaSeg leads to a significant performance boost on ADE20k semantic: **+6.1 mIoU** and **+5.1 mIoU** with ResNet50 and ViTDet-B backbones, respectively. This proves our argument that cotraining on more data helps overcome the data limitation issue of smaller-scale segmentation datasets.

4.2 DaTaSeg enables weakly-supervised transfer

In Table 1 (right), we evaluate DaTaSeg on ADE20k panoptic and Objects365 instance segmentation tasks. Note we only have weak supervision (ADE20k semantic and Objects365 bbox) during training. Again, we compare to models separately trained on one dataset as our baselines. Specifically, we use the ADE semantic for ADE panoptic evaluation, and an Objects365 model trained only using weak supervision for Objects365 instance evaluation, respectively.

By cotraining DaTaSeg in a multi-dataset multi-task fashion, we improve the ADE20k panoptic performance by **+2.9 PQ** and **+5.4 PQ** with ResNet50 and ViTDet-B backbones. Our design allows the panoptic segmentation knowledge to transfer from COCO to ADE20k. For reference, the fully-supervised performance is 37.7 PQ on ResNet50 and 42.3 PQ on ViTDet-B.

On Objects365, we only train with a weak box consistency loss \mathcal{L}_{proj} . The multi-dataset multi-task training recipe improves the mask AP by **+2.0 AP** and **+1.4 AP** for the two backbones. The improvement is most likely from the instance segmentation knowledge in COCO panoptic.

4.3 DaTaSeg scales with size of backbones

Our DaTaSeg design is orthogonal to detailed network architectures, as long as it is able to output the universal representation (binary mask proposals with class predictions). This is supported by

Method	Backbone	Training data	PC-59 mIoU	PC-459 mIoU	COCO mIoU	Cityscapes PQ
ODISE [63]	UNet+M2F	LAION+CLIP+COCO	55.3	13.8	52.4	23.9
MaskCLIP [12]	R-50	COCO pan+CLIP	45.9	10.0	–	–
OVSeg [35]	R-101c	COCO stuff+cap	53.3	11.0	–	–
	Swin-B		55.7	12.4	–	–
OpenSeg [15]	R-101	COCO pan+cap	42.1	9.0	36.1	–
	Eff-b7	COCO+Loc. Narr.	44.8	11.5	38.0	–
DaTaSeg	R-50	COCO panoptic	50.9	11.1	57.7	30.0
	ViTDet-B	+ADE semantic	51.1	11.6	62.7	28.0
	ViTDet-L	+O365 bbox	51.4	11.1	62.9	29.8

Table 3: **Compare DaTaSeg to state-of-the-art open-vocabulary segmentation models.** We apply DaTaSeg directly to other semantic or panoptic segmentation datasets without finetuning. We compare to ODISE [63], MaskCLIP [12], OVSeg [35], and OpenSeg [15] on their corresponding benchmarks. We only conduct system-level comparison due to differences in training data and backbones. DaTaSeg performs comparably on all semantic segmentation benchmarks and outperforms the recent work ODISE on Cityscapes. PC: Pascal Context. COCO: COCO is included in the training set for all models, and is not completely “open-vocabulary”.

# queries		50	100	150
ADE semantic	mIoU	47.4	48.1	48.7
COCO panoptic	PQ	48.7	49.0	48.9
ADE panoptic [†]	PQ	30.7	29.8	29.1
O365 instance [†]	AP	13.4	14.3	15.8

Table 4: **In general, the performance of DaTaSeg increases as we increase the number of segment queries.** Besides, using only 50 queries already achieves good performance. Experiments are conducted using a ResNet50 backbone. [†]: weakly-supervised tasks.

		DaTaSeg	+D-S modules
ADE semantic	mIoU	48.1	48.1 (-0.0)
COCO panoptic	PQ	49.0	46.0 (-3.0)
ADE panoptic [†]	PQ	29.8	26.9 (-2.9)
O365 instance [†]	AP	14.3	10.9 (-3.4)

Table 5: **Adding dataset-specific (D-S) modules hurt performance on almost all datasets.** This shows the importance of sharing all parameters for better knowledge sharing, which particularly benefits the weakly-supervised tasks. Experiments are conducted on a ResNet50 backbone.

the consistent performance gains among ResNet50, ViTDet-B, and ViTDet-L backbones as shown in Table 1. It also scales well as we increase the sizes of the backbones. With ViTDet-L, DaTaSeg reaches **53.5 mIoU** on ADE20k semantic and **54.0 PQ** on COCO panoptic in a single model.

4.4 DaTaSeg scales with number of datasets

We study how DaTaSeg scales with the number of training datasets. We train DaTaSeg on all combinations of one, two, and three datasets among the ADE20k semantic, COCO panoptic, and Objects365 detection datasets, in order to conduct a comprehensive study. Table 2 presents the results. Looking at each column, we see that performance on each dataset generally improves as the number of training datasets increases, especially for ADE semantic.

Since DaTaSeg shares all parameters among all datasets and tasks, we can evaluate the cross-dataset transfer performance. We notice the model transfers to datasets that are not trained. *e.g.*, A model trained on COCO panoptic and Objects365 detection achieves **18.3 mIoU** on ADE semantic, which is comparable to open-vocabulary segmentation performance (18.0 LSeg+ [15] with ResNet101).

4.5 DaTaSeg enables open-vocabulary segmentation

A further advantage of our fully-shared architecture is that we have the ability to directly transfer to other segmentation datasets. We simply switch the text embedding classifier with the vocabularies in a target dataset not used for training. Table 3 shows the results comparing DaTaSeg to several open-vocabulary works: ODISE [63] and MaskCLIP [12] are open-vocabulary panoptic segmentation methods and OVSeg [35] and OpenSeg [15] are open-vocabulary semantic segmentation approaches. Unlike these works, our method does not train on large-scale image-text data or use pretrained image-text models (except the pretrained text encoder), which puts our method at a disadvantage. Despite this disadvantage, DaTaSeg outperforms ODISE on the Cityscapes panoptic dataset. Note that there is a domain gap between our training sets and Cityscapes, which focuses on urban street scenes. DaTaSeg achieves comparable performance on PC-59 and PC-459. All methods in comparison train on COCO panoptic and ours has the best performance on COCO semantic. These results show that DaTaSeg enables open-vocabulary segmentation via our multi-dataset multi-task training approach.

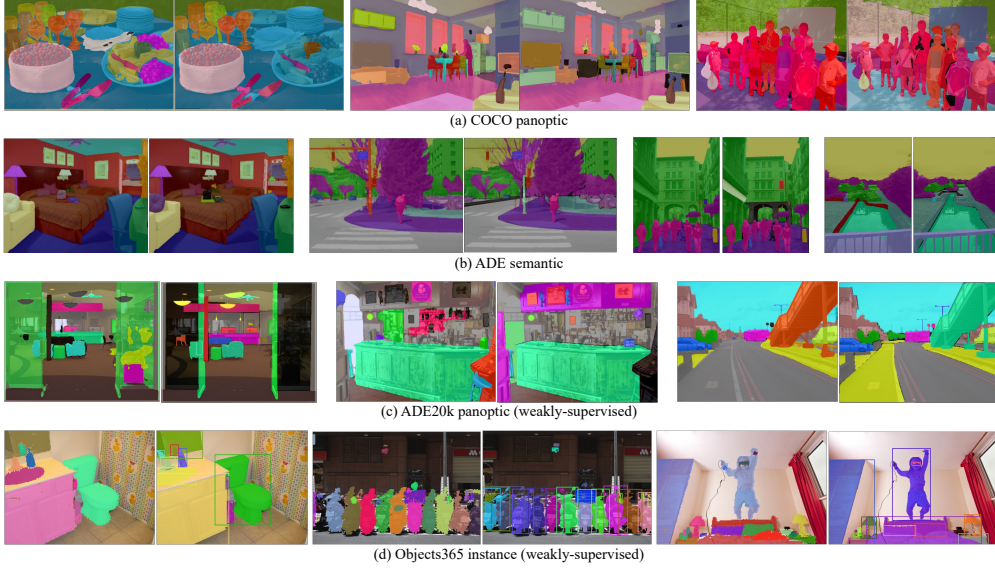


Figure 4: **Qualitative results of DaTaSeg on all datasets & tasks.** For every pair of images, the left is DaTaSeg prediction and the right is groundtruth. DaTaSeg succeeds on hard cases (*e.g.*, transparent wine glasses on the top left) as well as weakly-supervised datasets. For object instances in panoptic and instance segmentation, the colors are not matched to the groundtruths. Black denotes ignored regions.

4.6 DaTaSeg scales with number of queries

We perform ablation study on the number of segment queries Q_s and show the results in Table 4. The performance improves as we increase the number of queries from 50 to 150, on all datasets except ADE20k panoptic. Besides, DaTaSeg achieves reasonably good performance with only 50 queries, which may benefit memory-limited application scenarios.

4.7 Adding dataset-specific modules hurts performance

In multi-dataset learning, prior works have introduced dataset-specific modules [42], in order to address inconsistencies across datasets [31, 56]. However, such a design may weaken knowledge sharing across different datasets and tasks. This is especially so for weakly-supervised tasks which may rely more on other datasets and tasks to compensate for the weak supervision. To study this issue thoroughly, we carefully design several dataset-specific modules, including dataset-specific queries, dataset-specific heads, and dataset-specific prompts. These modules are lightweight by design so as to still encourage knowledge sharing through other shared parameters.

In Table 5, we evaluate the effectiveness of these dataset-specific modules by adding them to DaTaSeg, and keeping all other settings the same. Comparing with DaTaSeg that shares all parameters, results reveal that using dataset-specific modules hurts performance on all datasets except ADE20k semantic. Moreover, we see that the performance drops more on weakly-supervised tasks (ADE panoptic and O365 instance). This verifies that removing dataset-specific modules yields better knowledge sharing across datasets and tasks, and thus greatly improves performance. See supplementary for model details.

4.8 Qualitative analysis

We show qualitative results (with ViTDet-L) in Fig. 4. DaTaSeg performs well in both fully and weakly-supervised settings. We observe that localization quality is in general good, while classification is more error-prone. Nevertheless, DaTaSeg succeeds in challenging cases including transparent objects, occlusion, and crowd scenes.

5 Conclusion

The goal of our work is to train a single universal model on multiple datasets and multiple segmentation tasks (*i.e.*, semantic, instance and panoptic segmentation). We present DaTaSeg, which leverages a universal segmentation representation and shared semantic embedding space for classification. DaTaSeg surpasses separately trained models, leading to especially significant gains for smaller datasets such as ADE20k semantic. It unlocks a new weakly-supervised transfer capability on datasets that were not explicitly trained for a particular task (*e.g.*, ADE20k panoptic and Objects365 instance). DaTaSeg also directly transfer to more segmentation datasets and enables open-vocabulary segmentation. We believe that in the future, this multi-task multi-dataset setting will be the norm rather than the outlier as it currently is, and we see our paper as taking a step in this direction.

References

- [1] Jimmy Lei Ba, Jamie Ryan Kiros, and Geoffrey E Hinton. Layer normalization. *arXiv preprint arXiv:1607.06450*, 2016. 6
- [2] Rodrigo Benenson, Stefan Popov, and Vittorio Ferrari. Large-scale interactive object segmentation with human annotators. In *CVPR*, 2019. 6
- [3] Maxime Bucher, Tuan-Hung Vu, Matthieu Cord, and Patrick Pérez. Zero-shot semantic segmentation. *NeurIPS*, 2019. 14
- [4] Nicolas Carion, Francisco Massa, Gabriel Synnaeve, Nicolas Usunier, Alexander Kirillov, and Sergey Zagoruyko. End-to-end object detection with transformers. In *ECCV*, 2020. 6
- [5] Liang-Chieh Chen, George Papandreou, Iasonas Kokkinos, Kevin Murphy, and Alan L Yuille. Deeplab: Semantic image segmentation with deep convolutional nets, atrous convolution, and fully connected crfs. *TPAMI*, 2017. 1, 3
- [6] Bowen Cheng, Maxwell D Collins, Yukun Zhu, Ting Liu, Thomas S Huang, Hartwig Adam, and Liang-Chieh Chen. Panoptic-DeepLab: A Simple, Strong, and Fast Baseline for Bottom-Up Panoptic Segmentation. In *CVPR*, 2020. 3
- [7] Bowen Cheng, Ishan Misra, Alexander G Schwing, Alexander Kirillov, and Rohit Girdhar. Masked-attention mask transformer for universal image segmentation. In *CVPR*, 2022. 1, 3, 5, 18, 19
- [8] Bowen Cheng, Omkar Parkhi, and Alexander Kirillov. Pointly-supervised instance segmentation. In *CVPR*, 2022. 18
- [9] Bowen Cheng, Alex Schwing, and Alexander Kirillov. Per-pixel classification is not all you need for semantic segmentation. *NeurIPS*, 2021. 1, 2, 3, 6
- [10] Marius Cordts, Mohamed Omran, Sebastian Ramos, Timo Rehfeld, Markus Enzweiler, Rodrigo Benenson, Uwe Franke, Stefan Roth, and Bernt Schiele. The cityscapes dataset for semantic urban scene understanding. In *CVPR*, 2016. 2, 6
- [11] Jifeng Dai, Kaiming He, and Jian Sun. Boxsup: Exploiting bounding boxes to supervise convolutional networks for semantic segmentation. In *ICCV*, 2015. 3
- [12] Zheng Ding, Jieke Wang, and Zhuowen Tu. Open-vocabulary panoptic segmentation with maskclip. *arXiv preprint arXiv:2208.08984*, 2022. 8
- [13] Mark Everingham, Luc Van Gool, Christopher KI Williams, John Winn, and Andrew Zisserman. The pascal visual object classes (voc) challenge. *IJCV*, 2010. 14
- [14] Golnaz Ghiasi, Yin Cui, Aravind Srinivas, Rui Qian, Tsung-Yi Lin, Ekin D Cubuk, Quoc V Le, and Barret Zoph. Simple copy-paste is a strong data augmentation method for instance segmentation. In *Proceedings of the IEEE/CVF conference on computer vision and pattern recognition*, 2021. 19
- [15] Golnaz Ghiasi, Xiuye Gu, Yin Cui, and Tsung-Yi Lin. Scaling open-vocabulary image segmentation with image-level labels. In *ECCV*, 2022. 5, 6, 8
- [16] Zhangxuan Gu, Siyuan Zhou, Li Niu, Zihan Zhao, and Liqing Zhang. Context-aware feature generation for zero-shot semantic segmentation. In *ACM MM*, 2020. 14

- [17] Agrim Gupta, Piotr Dollar, and Ross Girshick. Lvis: A dataset for large vocabulary instance segmentation. In *CVPR*, 2019. 14
- [18] Bharath Hariharan, Pablo Arbeláez, Ross Girshick, and Jitendra Malik. Simultaneous detection and segmentation. In *ECCV*, 2014. 1, 3
- [19] Kaiming He, Xinlei Chen, Saining Xie, Yanghao Li, Piotr Dollár, and Ross Girshick. Masked autoencoders are scalable vision learners. In *CVPR*, 2022. 6
- [20] Kaiming He, Georgia Gkioxari, Piotr Dollár, and Ross Girshick. Mask r-cnn. In *ICCV*, 2017. 1, 3
- [21] Kaiming He, Xiangyu Zhang, Shaoqing Ren, and Jian Sun. Deep residual learning for image recognition. In *CVPR*, 2016. 2, 6
- [22] Xuming He, Richard S Zemel, and Miguel Á Carreira-Perpiñán. Multiscale conditional random fields for image labeling. In *CVPR*, 2004. 1
- [23] Dan Hendrycks and Kevin Gimpel. Gaussian error linear units (gelus). *arXiv preprint arXiv:1606.08415*, 2016. 6
- [24] Jitesh Jain, Jiachen Li, MangTik Chiu, Ali Hassani, Nikita Orlov, and Humphrey Shi. Oneformer: One transformer to rule universal image segmentation. In *CVPR*, 2023. 1, 3
- [25] Anna Khoreva, Rodrigo Benenson, Jan Hosang, Matthias Hein, and Bernt Schiele. Simple does it: Weakly supervised instance and semantic segmentation. In *CVPR*, 2017. 3
- [26] Dongwan Kim, Yi-Hsuan Tsai, Yumin Suh, Masoud Faraki, Sparsh Garg, Manmohan Chandraker, and Bohyung Han. Learning semantic segmentation from multiple datasets with label shifts. In *ECCV*, 2022. 1, 2
- [27] Alexander Kirillov, Ross Girshick, Kaiming He, and Piotr Dollár. Panoptic feature pyramid networks. In *CVPR*, 2019. 1, 3
- [28] Alexander Kirillov, Kaiming He, Ross Girshick, Carsten Rother, and Piotr Dollár. Panoptic segmentation. In *CVPR*, 2019. 1, 2, 3, 6
- [29] Harold W Kuhn. The hungarian method for the assignment problem. *Naval research logistics quarterly*, 1955. 4
- [30] Viveka Kulharia, Siddhartha Chandra, Amit Agrawal, Philip Torr, and Amrith Tyagi. Box2seg: Attention weighted loss and discriminative feature learning for weakly supervised segmentation. In *ECCV*, 2020. 3
- [31] John Lambert, Zhuang Liu, Ozan Sener, James Hays, and Vladlen Koltun. Mseg: A composite dataset for multi-domain semantic segmentation. In *CVPR*, 2020. 1, 2, 5, 9, 16
- [32] Shiyi Lan, Zhiding Yu, Christopher Choy, Subhashree Radhakrishnan, Guilin Liu, Yuke Zhu, Larry S Davis, and Anima Anandkumar. Discobox: Weakly supervised instance segmentation and semantic correspondence from box supervision. In *ICCV*, 2021. 3
- [33] Qizhu Li, Anurag Arnab, and Philip HS Torr. Weakly-and semi-supervised panoptic segmentation. In *ECCV*, 2018. 3
- [34] Yanghao Li, Hanzi Mao, Ross Girshick, and Kaiming He. Exploring plain vision transformer backbones for object detection. In *ECCV*, 2022. 2, 6
- [35] Feng Liang, Bichen Wu, Xiaoliang Dai, Kunpeng Li, Yinan Zhao, Hang Zhang, Peizhao Zhang, Peter Vajda, and Diana Marculescu. Open-vocabulary semantic segmentation with mask-adapted clip. *arXiv preprint arXiv:2210.04150*, 2022. 8
- [36] Valerii Likhoshesterov, Anurag Arnab, Krzysztof Choromanski, Mario Lucic, Yi Tay, Adrian Weller, and Mostafa Dehghani. Polyvit: Co-training vision transformers on images, videos and audio. *arXiv preprint arXiv:2111.12993*, 2021. 6
- [37] Di Lin, Jifeng Dai, Jiaya Jia, Kaiming He, and Jian Sun. Scribblesup: Scribble-supervised convolutional networks for semantic segmentation. In *CVPR*, 2016. 3
- [38] Tsung-Yi Lin, Piotr Dollár, Ross Girshick, Kaiming He, Bharath Hariharan, and Serge Belongie. Feature pyramid networks for object detection. In *CVPR*, 2017. 6, 18

- [39] Tsung-Yi Lin, Priya Goyal, Ross Girshick, Kaiming He, and Piotr Dollár. Focal loss for dense object detection. In *ICCV*, 2017. 6
- [40] Jonathan Long, Evan Shelhamer, and Trevor Darrell. Fully convolutional networks for semantic segmentation. In *CVPR*, 2015. 1, 3
- [41] Ilya Loshchilov and Frank Hutter. Decoupled weight decay regularization. *ICLR*, 2019. 19
- [42] Lingchen Meng, Xiyang Dai, Yinpeng Chen, Pengchuan Zhang, Dongdong Chen, Mengchen Liu, Jianfeng Wang, Zuxuan Wu, Lu Yuan, and Yu-Gang Jiang. Detection hub: Unifying object detection datasets via query adaptation on language embedding. *arXiv preprint arXiv:2206.03484*, 2022. 2, 9
- [43] Fausto Milletari, Nassir Navab, and Seyed-Ahmad Ahmadi. V-net: Fully convolutional neural networks for volumetric medical image segmentation. In *3DV. Ieee*, 2016. 5, 6
- [44] Roozbeh Mottaghi, Xianjie Chen, Xiaobai Liu, Nam-Gyu Cho, Seong-Whan Lee, Sanja Fidler, Raquel Urtasun, and Alan Yuille. The role of context for object detection and semantic segmentation in the wild. In *CVPR*, 2014. 2, 6
- [45] George Papandreou, Liang-Chieh Chen, Kevin P Murphy, and Alan L Yuille. Weakly-and semi-supervised learning of a deep convolutional network for semantic image segmentation. In *ICCV*, 2015. 3
- [46] Giuseppe Pastore, Fabio Cermelli, Yongqin Xian, Massimiliano Mancini, Zeynep Akata, and Barbara Caputo. A closer look at self-training for zero-label semantic segmentation. In *CVPRW*, 2021. 14
- [47] Siyuan Qiao, Liang-Chieh Chen, and Alan Yuille. Detectors: Detecting objects with recursive feature pyramid and switchable atrous convolution. In *CVPR*, 2021. 3
- [48] Alec Radford, Jong Wook Kim, Chris Hallacy, Aditya Ramesh, Gabriel Goh, Sandhini Agarwal, Girish Sastry, Amanda Askell, Pamela Mishkin, Jack Clark, et al. Learning transferable visual models from natural language supervision. In *ICML*, 2021. 6
- [49] Tal Remez, Jonathan Huang, and Matthew Brown. Learning to segment via cut-and-paste. In *ECCV*, 2018. 3
- [50] Olga Russakovsky, Jia Deng, Hao Su, Jonathan Krause, Sanjeev Satheesh, Sean Ma, Zhiheng Huang, Andrej Karpathy, Aditya Khosla, Michael S. Bernstein, Alexander C. Berg, and Li Fei-Fei. Imagenet large scale visual recognition challenge. *IJCV*, 115:211–252, 2015. 6
- [51] Shuai Shao, Zeming Li, Tianyuan Zhang, Chao Peng, Gang Yu, Xiangyu Zhang, Jing Li, and Jian Sun. Objects365: A large-scale, high-quality dataset for object detection. In *ICCV*, 2019. 2, 6
- [52] Yunhang Shen, Liujuan Cao, Zhiwei Chen, Feihong Lian, Baochang Zhang, Chi Su, Yongjian Wu, Feiyue Huang, and Rongrong Ji. Toward joint thing-and-stuff mining for weakly supervised panoptic segmentation. In *CVPR*, 2021. 3
- [53] Chunfeng Song, Yan Huang, Wanli Ouyang, and Liang Wang. Box-driven class-wise region masking and filling rate guided loss for weakly supervised semantic segmentation. In *CVPR*, 2019. 3
- [54] Zhi Tian, Chunhua Shen, Xinlong Wang, and Hao Chen. Boxinst: High-performance instance segmentation with box annotations. In *CVPR*, 2021. 3
- [55] Zhi Tian, Chunhua Shen, Xinlong Wang, and Hao Chen. Boxinst: High-performance instance segmentation with box annotations. In *CVPR*, 2021. 4, 5
- [56] Jasper Uijlings, Thomas Mensink, and Vittorio Ferrari. The missing link: Finding label relations across datasets. In *ECCV*, 2022. 2, 9, 16
- [57] Ashish Vaswani, Noam Shazeer, Niki Parmar, Jakob Uszkoreit, Llion Jones, Aidan N Gomez, Łukasz Kaiser, and Illia Polosukhin. Attention is all you need. *NeurIPS*, 2017. 6
- [58] Huiyu Wang, Yukun Zhu, Hartwig Adam, Alan Yuille, and Liang-Chieh Chen. Max-deeplab: End-to-end panoptic segmentation with mask transformers. In *CVPR*, 2021. 1, 2, 3
- [59] Xudong Wang, Zhaowei Cai, Dashan Gao, and Nuno Vasconcelos. Towards universal object detection by domain attention. In *CVPR*, 2019. 2
- [60] Yongqin Xian, Subhabrata Choudhury, Yang He, Bernt Schiele, and Zeynep Akata. Semantic projection network for zero-and few-label semantic segmentation. In *CVPR*, 2019. 14

- [61] Yuwen Xiong, Renjie Liao, Hengshuang Zhao, Rui Hu, Min Bai, Ersin Yumer, and Raquel Urtasun. Upsnet: A unified panoptic segmentation network. In *CVPR*, 2019. 3
- [62] Hang Xu, Linpu Fang, Xiaodan Liang, Wenxiong Kang, and Zhenguo Li. Universal-rcnn: Universal object detector via transferable graph r-cnn. In *AAAI*, 2020. 2
- [63] Jiarui Xu, Sifei Liu, Arash Vahdat, Wonmin Byeon, Xiaolong Wang, and Shalini De Mello. Open-vocabulary panoptic segmentation with text-to-image diffusion models. *CVPR*, 2023. 8
- [64] Tien-Ju Yang, Maxwell D Collins, Yukun Zhu, Jyh-Jing Hwang, Ting Liu, Xiao Zhang, Vivienne Sze, George Papandreou, and Liang-Chieh Chen. Deeperlab: Single-shot image parser. *arXiv preprint arXiv:1902.05093*, 2019. 3
- [65] Qihang Yu, Huiyu Wang, Siyuan Qiao, Maxwell Collins, Yukun Zhu, Hartwig Adam, Alan Yuille, and Liang-Chieh Chen. k-means Mask Transformer. In *ECCV*, 2022. 3
- [66] Hongyi Zhang, Moustapha Cisse, Yann N Dauphin, and David Lopez-Paz. mixup: Beyond empirical risk minimization. *ICLR*, 2018. 19
- [67] Wenwei Zhang, Jiangmiao Pang, Kai Chen, and Chen Change Loy. K-net: Towards unified image segmentation. *NeurIPS*, 2021. 1, 3
- [68] Bolei Zhou, Hang Zhao, Xavier Puig, Sanja Fidler, Adela Barriuso, and Antonio Torralba. Scene parsing through ade20k dataset. In *CVPR*, 2017. 2, 6
- [69] Chong Zhou, Chen Change Loy, and Bo Dai. Denseclip: Extract free dense labels from clip. *ECCV*, 2022. 14
- [70] Qiang Zhou, Yang Liu, Chaohui Yu, Jingliang Li, Zhibin Wang, and Fan Wang. Lmseg: Language-guided multi-dataset segmentation. *arXiv preprint arXiv:2302.13495*, 2023. 1, 2
- [71] Xingyi Zhou, Vladlen Koltun, and Philipp Krähenbühl. Simple multi-dataset detection. In *CVPR*, 2022. 2
- [72] Xizhou Zhu, Weiye Su, Lewei Lu, Bin Li, Xiaogang Wang, and Jifeng Dai. Deformable detr: Deformable transformers for end-to-end object detection. In *ICLR*, 2021. 18

Appendix

A Broader Impacts

We propose a single framework for multi-dataset multi-task segmentation, which especially benefits memory-limited application scenarios, *e.g.*, our work can make a single segmentation model that meets all kinds of segmentation needs on memory-limited mobile devices (semantic segmentation for photo editing, instance segmentation for object detection and image search, *etc.*), instead of using separate models for various segmentation tasks.

Moreover, our approach improves segmentation performance from a data-centric view: We leverage segmentation data from multiple sources to improve the overall segmentation performance, especially on datasets of smaller scales, *e.g.*, ADE20k semantic. We also transfer knowledge from other sources to enable weakly-supervised segmentation. This is helpful on the scenario where segmentation data are very hard to collect, we can cotrain on similar data to help improve the performance, or even train on data with weaker supervision. *e.g.*, if we want to train a segmentation model on rare wild animals, we can co-train a model on a small set of these kinds of animals, and a larger dataset of more common animals.

As for biases and fairness, our model learns from the training data, so it may inherit the biases and fairness issues existing in the training data. Nonetheless, our model trains on multiple sources, and the datasets with less biases and fairness issues may compensate the biases and fairness issues in other datasets.

Method	Backbone	mIoU	mIoU-unseen	mIoU-seen
SPNet [60]		56.9	0.0	75.8
SPNet-C [60]		63.2	15.6	78.0
ZS3Net [3]		61.6	17.7	77.3
CaGNet [16]	DeepLabv2-ResNet101	65.5	26.6	78.4
STRICT [46]		70.9	35.6	82.7
DenseCLIP+ [69]		88.1	86.1	88.8
Fully-supervised		88.2	87.0	88.6
DaTaSeg	ResNet-50	89.4	87.7	89.9
	ViTDet-B	92.8	90.9	93.4
	ViTDet-L	94.7	94.3	94.9

Table 6: **Comparison with zero-shot segmentation methods on PASCAL VOC 2012 segmentation dataset.** DaTaSeg with a ResNet-50 backbone already outperforms all other methods. Note that zero-shot methods are trained on 15 seen classes of PASCAL VOC and only 5 classes are unseen (mIoU-unseen). In contrast, DaTaSeg has never seen PASCAL VOC images during training (it’s trained on several other datasets). Following [69], the background class is ignored. The numbers of the comparison methods are from [69]. SPNet-C stands for SPNet with calibration.

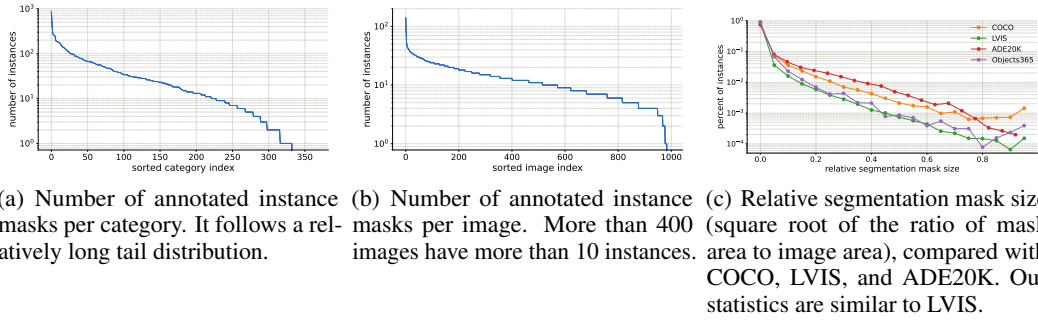


Figure 5: **Dataset statistics for our Objects365 instance segmentation validation set.**

B Comparison with zero-shot segmentation on PASCAL VOC

We evaluate DaTaSeg on the PASCAL VOC 2012 semantic segmentation dataset [13], which includes 20 object classes and a background class. We directly transfer our trained model to its validation set with 1,449 images. We follow the setting in DenseCLIP [69] and ignore the background class during evaluation.

We compare with other zero-shot segmentation methods in Table 6, which are trained on 15 seen classes with 5 classes held out during training as unseen classes (potted plant, sheep, sofa, train, and TV monitor). DaTaSeg has never seen the entire PASCAL VOC dataset during training, though it is trained on other segmentation datasets (COCO panoptic, ADE semantic, and Objects365 detection). DaTaSeg with a ResNet-50 backbone outperforms all zero-shot methods with DeepLabv2-ResNet101 backbones, on all categories. Surprisingly, DaTaSeg even outperforms the fully-supervised counterpart. We note this is not an apple-to-apple comparison, since the training sources are different. The main purpose of this comparison is to show how our “data-centric” DaTaSeg is positioned against zero-shot segmentation methods on the PASCAL VOC dataset, using a direct transfer manner.

C More about our newly labeled Objects365 instance segmentation validation dataset

We randomly sampled 1,000 images from the Objects365 V2 validation set. Different from the “federated” LVIS dataset [17] (not all categories in each image are completely labeled), the bounding boxes in Objects365 are completely labeled for each image and we follow this complete annotation for the instance masks. For each bounding box annotation, we generate a foreground/background annotation question for the raters. In the question, raters are asked to paint the instance mask on the original image, with the groundtruth bbox shown on the image as a guide and the groundtruth category displayed on the side. We do not crop the original image to the bbox region, but show the entire image to provide more context information, which is especially helpful for small objects. If the boundary is too blurry or too dark to annotate the instance mask, the raters can skip the question.



Figure 6: **Visualization of our Objects365 instance segmentation dataset.** We store binary masks, which has higher accuracy compared with polygons. The quality on small objects are good (first two images). Complex structures are also labeled delicately, *e.g.*, the camels (1st image on 2nd row) and the decoration on the cake (1st image on 3rd row). For occlusions, raters carefully avoid the occluded regions as they are not a part of the object to annotate, *e.g.*, the fruits in the basket are not included in the basket masks (last image on 1st row).

The annotation tool is a free painting tool, which allows the raters to freely draw the instance mask. We ask the raters to try to draw within the bbox, but if the object is obviously exceeding the bbox, then they can draw outside the bbox. The size of the stroke is adjustable. Raters can zoom-in/out, draw straight lines, and fill the inside of a plotted boundary (which is quite useful for instance segmentation). Unlike polygons in COCO *etc.*, our tool saves binary masks for higher-resolution masks.

We inserted a total of 13,372 questions (we do not label the crowd instances, as they are skipped in both training and validation following the common practice in instance segmentation), and we obtained 12,836 valid instance mask annotations. It takes a total of 800.59 rater hours. On average, raters spend 3.74 minutes on each valid mask.

In Fig. 5, we show some statistics about our Objects365 instance segmentation dataset. The number of masks per category follows a relatively long-tailed distribution (Fig. 5(a)). The number of masks per image reveals that a large number of images have many instance annotations (Fig. 5(b)). And the statistics of the relative mask size is close to that of the LVIS datasets (Fig. 5(c)).

As shown in Fig. 6, we visualized the mask annotations and they are very high-quality. The raters carefully handled small objects, thin structures, complicated shapes, occluded objects, *etc.*

For the objects who do not have an instance mask since raters skipped it, it's possible that the model still predicts an instance mask for that object. We do not want to treat such cases as false positive, so we ignore them during evaluation.

We'll release this dataset. We believe this efforts can provide the community a good benchmark for instance segmentation evaluation, *e.g.*, for evaluating weakly-supervised instance segmentation learned from bounding boxes.

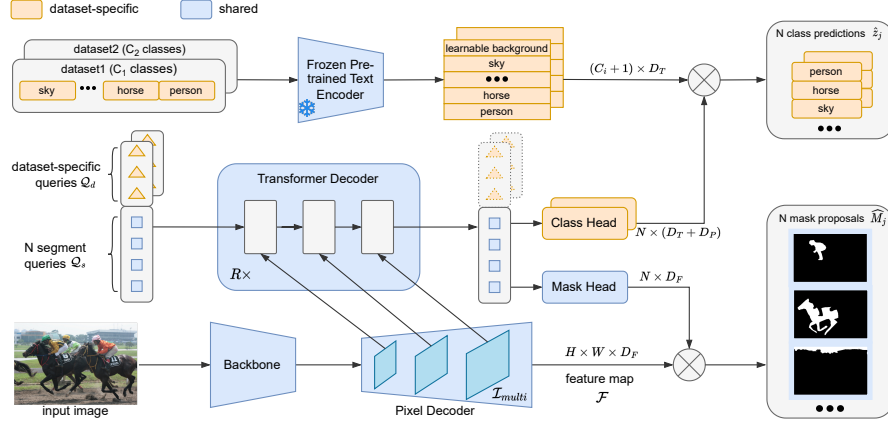


Figure 8: **Overview of incorporating all our designed dataset-specific modules into our universal multi-dataset multi-task segmentation model (DaTaSeg).** We design a set of *dataset-specific queries* fed into the transformer decoder, *dataset-specific classification head*, and *dataset-specific background classifier*. They are highlighted in orange. All these modules are learnable. Different datasets have separate parameters for these modules.

# of dataset-specific queries	fully-supervised		weakly-supervised transfer	
	ADE	COCO	ADE	O365
	semantic mIoU	panoptic PQ	semantic → panoptic PQ	box → instance mask AP
0	47.8	48.1	28.6	13.1
10	48.0	46.2	28.0	11.2
20	48.6	46.6	28.5	11.7
30	47.1	45.8	27.4	11.7

Table 7: **Ablation study on the number of dataset-specific queries Q_d .** Evaluated on a ResNet50 backbone. Without dataset-specific queries, the performance on COCO panoptic and Objects365 instance segmentation is much better. Using a large number of dataset-specific queries, e.g., 30, hurts performance on many datasets, since it weakens knowledge sharing among datasets & tasks.

Overall architecture: The overall architecture equipped with all our dataset-specific modules is shown in Fig. 8. We design the dataset-specific modules to be light-weight, which allows us to save on memory costs. With this design of a mixture of a mostly shared network and light-weight dataset-specific modules, the model has the freedom to choose whether to leverage dataset-specific information, or to use the shared knowledge across datasets/tasks. However, one significant disadvantage of adding dataset-specific modules is it’s hard to decide which set of dataset-specific parameters to use when directly transferring to other datasets (Sec. 4.5), and thus it *hurts the open-vocabulary capability*.

Ablation studies on dataset-specific modules: We ablate on the number of dataset-specific queries Q_d in Table 7. It shows that removing the dataset-specific queries achieves the best results on COCO panoptic and Objects365 by a large margin. It also achieves reasonable performance on other datasets. Using 30 queries hurts the performance on COCO panoptic and ADE semantic.

In Table 8, we compare using and not using dataset-specific classification modules (the classification embedding head and background classifier). Results indicate that removing dataset-specific classification improves performance on all datasets & tasks, especially the weakly-supervised tasks. We suspect it’s because weakly-supervised tasks rely more on knowledge sharing.

System-level comparison between with and without dataset-specific modules: In the main paper, due to space limit, we only show results of adding all dataset-specific modules on a ResNet50 backbone. In Table 9, we show the same comparison on more backbones, i.e., ResNet50, ViTDet-B, and ViTDet-L. The observation is consistent across all backbones: adding dataset-specific modules hurts performance on all datasets. The difference is more significant on backbones of smaller scales, and on COCO panoptic and Objects365 instance segmentation datasets.

		w/ dataset-specific classification	w/o dataset-specific classification
ADE semantic	mIoU	47.9	48.1 (+0.2)
COCO panoptic	PQ	48.5	49.0 (+0.5)
ADE panoptic [†]	PQ	28.7	29.8 (+1.1)
O365 instance [†]	AP	12.9	14.3 (+1.4)

Table 8: **Adding dataset-specific classification modules hurt performance on almost all datasets.** The dataset-specific classification modules include the classification embedding head and the learnable background classifier. Evaluated on a ResNet50 backbone, without other dataset-specific modules.

Backbone	Model	Fully-Supervised		Weakly-Supervised Transfer	
		ADE	COCO	ADE	O365
		semantic mIoU	panoptic PQ	semantic → panoptic PQ	box → instance mask AP
ResNet50	+D-S modules	48.1	46.0	26.9	10.9
	DaTaSeg	48.1 (+0.0)	49.0 (+3.0)	29.8 (+2.9)	14.3 (+3.4)
ViTDet-B	+D-S modules	51.0	50.8	31.0	13.1
	DaTaSeg	51.4 (+0.4)	52.8 (+2.0)	32.9 (+1.9)	16.1 (+3.0)
ViTDet-L	+D-S modules	53.9	52.3	33.5	13.7
	DaTaSeg	54.0 (+0.1)	53.5 (+1.2)	33.4 (-0.1)	16.4 (+2.7)

Table 9: **Comparing DaTaSeg with the alternative architecture adding all dataset-specific modules on various backbones.** Results show that removing the dataset-specific modules improve performance on all datasets and all backbones. The gains are most significant on Objects365 instance and COCO panoptic segmentation (with dataset-specific modules, it cannot outperform the separately trained baseline on COCO panoptic).

E Architecture change from Mask2Former

Our network architecture is based on Mask2Former [7]. However, due to hardware difference (TPU vs. GPU), we need to make modifications to Mask2Former architecture to run on our hardware. Unlike GPUs, TPUs require a static computation graph with *fixed-shape* data (otherwise, it recompiles for each computation graph/change of data shape, and causes significant slowdown). Therefore, we drop all the TPU-unfriendly operations in Mask2Former. In particular, we change the *multi-scale deformable attention transformer* [72] pixel decoder to a plain FPN [38]. The performance comparison is shown in Table 4(e) in the Mask2Former paper (51.9 PQ of deformable-attention vs. 50.7 PQ of FPN on COCO panoptic). Also, we do not use the *sampled point loss* [8] in either the matching loss or the training loss calculation, and use the vanilla mask loss. The performance comparison is shown in Table 5 in the Mask2Former paper (51.9 PQ of point loss vs. 50.3 PQ of mask loss). Besides, we *do not use varying input size* during evaluation and use a fixed input size (first resize then pad).

To improve the training speed, we *modify the deep supervision* in the masked attention transformer decoder: for every decoder layer, we use the same matching indices computed from the outputs of the last decoder layer, but use a different prediction head. We *do not use the mask predictions from the initial queries* as attention masks, since the predictions are not made based on the input image.

F Additional implementation details

In addition to the implementation details described in Sec. 4, we provide more details here.

Preprocessing. In order to do 1:1 Hungarian matching, we preprocess the groundtruth into the same format as the predictions described in Sec. 3.2. In **panoptic segmentation**, we transfer the groundtruth into a set of binary masks with class labels. For “thing” categories, we group the pixels belonging to each instance into a separate groundtruth mask; for “stuff” categories, we group all pixels in each stuff category as the groundtruth mask. Similarly, in **semantic segmentation**, we group all pixels in each category as the groundtruth mask. For **instance segmentation**, since we are using bounding box weak supervision, we do not need this preprocessing step. For all mask proposal groundtruth, we downsample it by 4 times, to save memory cost during training.

Training settings. We randomly scale the input image in the range of [0.1, 2.0] and then pad or crop it to 1024×1024 . For ADE20k dataset, since the image size is smaller than other datasets, we use a

	μ_{ce}	μ_{focal}	μ_{dice}	μ_{proj}	λ_{ce}	λ_{focal}	λ_{dice}	λ_{proj}
ADE semantic	1	20	5	0	1	20	5	0
COCO panoptic	1	0	1	0	1	20	5	0
O365 instance (box GT)	1	0	0	0.5	1	0	0	2

Table 10: **The weights we use to compute the matching cost and total loss (Eq. 4,5 in the main paper) for all training datasets.** μ 's are for the matching cost and λ 's are for the total training loss.

scaling range of [0.5, 2.0]. We use the AdamW optimizer [41] with a weight decay of 0.05. We clip the gradients with a max norm of 0.1. The weight for the background class is set to 0.05 in \mathcal{L}_{ce} . The matching cost and loss weight settings for Eq. 4,5 in the main paper are shown in Table 10. We use a dataset sampling ratio of 1:4:4 for ADE semantic, COCO panoptic, and Objects detection. We adopt a different learning rate multiplier for each dataset: We multiply the learning rate on ADE semantic, COCO panoptic, and Objects365 detection by 3, 5, 2, respectively. On ResNet50 backbones, we use a batch size of 384 and train 500k iterations, with a learning rate of 3e-5. We adopt the step learning rate schedule: We multiply the learning rate by $0.1 \times$ at the 0.9 and 0.95 fractions of the total training iterations. On the ViTDet-B backbones, we train 600k iterations with a learning rate of 6e-5. On ViTDet-L, we use a batch size of 256 and train 540.5k iterations with a learning rate of 4e-5. For ResNet50, we train on 64 TPU v4 chips; for ViTDet backbones, we train on 128 TPU v4 chips. All evaluations are conducted on 4 GPUs with a batch size of 8.

Postprocessing. We first apply the MERGE operation described in Sec. 3.2. We follow the postprocessing operations in [7] with some modifications: In panoptic segmentation, we use a confidence threshold of 0.85 to filter mask proposals for COCO panoptic, and set the threshold to 0.8 for ADE panoptic. For panoptic and instance segmentation, we filter out final segments whose area is smaller than 4. For instance segmentation, we return a maximum of 100 instances per image with a score threshold of 0.0. For all tasks, the final scores are the production of classification scores and localization scores (binary mask classification).

G Limitations

Our proposed method is not without limitations. Since we are the first work to explore multi-dataset multi-task segmentation model, we do not introduce the complexity for an efficient framework. There are several ways to improve the model efficiency, *e.g.*, calculating the mask loss on sampled points only [7], while we do not deploy this in our framework, since it's not our key contribution. Moreover, as shown in the experiment section (Table 1), our framework is orthogonal to the detailed network architecture as long as the network is able to output our universal segmentation representation.

For weakly-supervised panoptic segmentation on ADE20k panoptic, we notice that sometimes multiple instances of the same category are not separated in the prediction. We believe using certain data augmentation techniques, *e.g.*, MixUp [66] and Copy-Paste [14], may farther enhance knowledge transfer between datasets of different tasks, and may thus help mitigate this issue. We leave it for future work to improve on these limitations.

H Additional qualitative results

We notice sometimes our predictions do not match the groundtruth, but it does not necessarily mean the predictions are not good. Fig. 9 shows two examples on COCO panoptic. On the left column, DaTaSeg does a better job in segmenting 'sky' and 'tree-merged' than the groundtruth. The classification of 'pavement-merged' is also better than 'dirt-merged', which is probably due to *language ambiguity*: the British meaning of 'pavement' is sidewalk, while the annotator may be more used to the North American usage of 'pavement'. On the right column, DaTaSeg predicts 'window-other', while the groundtruth is 'tree-merged' for the scene through the window, and both make sense due to *label ambiguity*. In addition, DaTaSeg is able to predict the 'mirror-stuff', 'shelf', 'light', 'bottle', and more 'book's, which are missing from the groundtruth.

We show qualitative results for the direct transfer experiments in Fig. 10,11,12,13, on PASCAL Context 59 (PC-59), PASCAL Context 459 (PC-459), COCO semantic, and Cityscapes panoptic datasets, respectively. These results serve as a supplementary material for Table 3 in the main paper. They show DaTaSeg directly transfer to other segmentation datasets unseen during training with

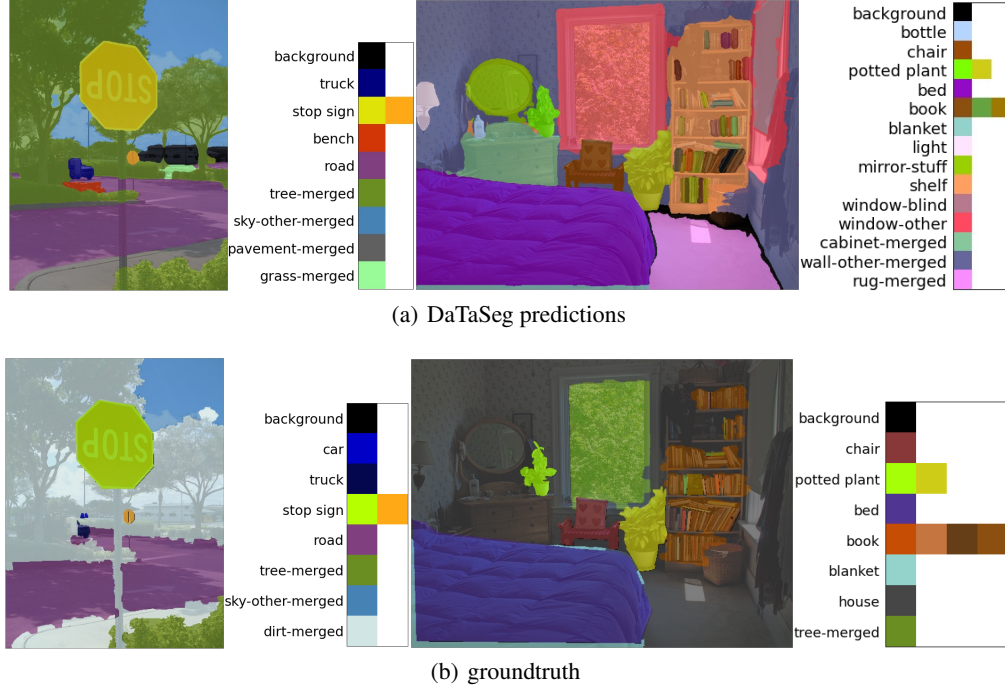


Figure 9: **Examples on COCO panoptic showing that sometimes DaTaSeg’s predictions do not match the groundtruth, but it does not necessarily mean they are wrong.** On the left, DaTaSeg’s prediction is ‘pavement-merged’, while the groundtruth is ‘dirt-merged’ (Probably because the British meaning of ‘pavement’ is sidewalk, while the annotator is more used to the North American meaning of ‘pavement’). Ours also segments ‘tree’ and ‘sky’ better. On the right, the definition for the scene through the window is ambiguous: ‘window-other’ (ours) v.s. ‘tree-merged’ (GT). The groundtruth misses to label several objects, while DaTaSeg recognizes more objects, *e.g.*, ‘mirror-stuff’, ‘light’, ‘shelf’, ‘bottle’. Legends for ‘book’ are truncated due to space limit.

high quality both in localization and classification. DaTaSeg performs well on large-vocabulary segmentation (PC-459), and handles hard cases well (thin structures, small objects, complicated scenes, occlusions, *etc.*).

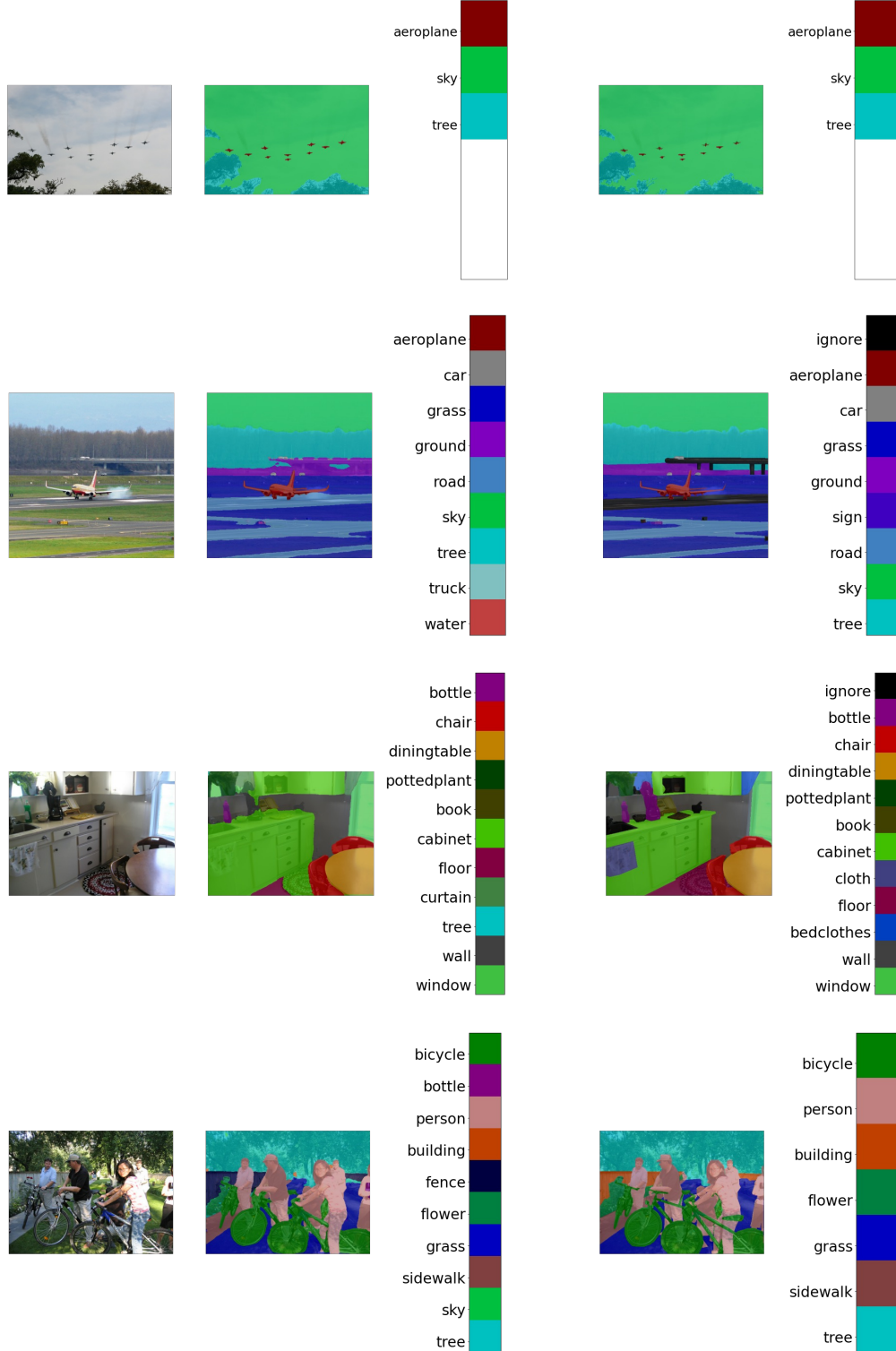


Figure 10: **Qualitative results of DaTaSeg directly transferring to PASCAL Context semantic dataset with 59 categories (PC-59).** The results demonstrate DaTaSeg has good generalization ability. The top row shows DaTaSeg is able to segment small objects (aeroplane), and the last row indicates DaTaSeg segments fine structures (bicycles) well. For each row, the left is the input image, the middle is our prediction, and the right is groundtruth. With a ViTDet-L backbone.

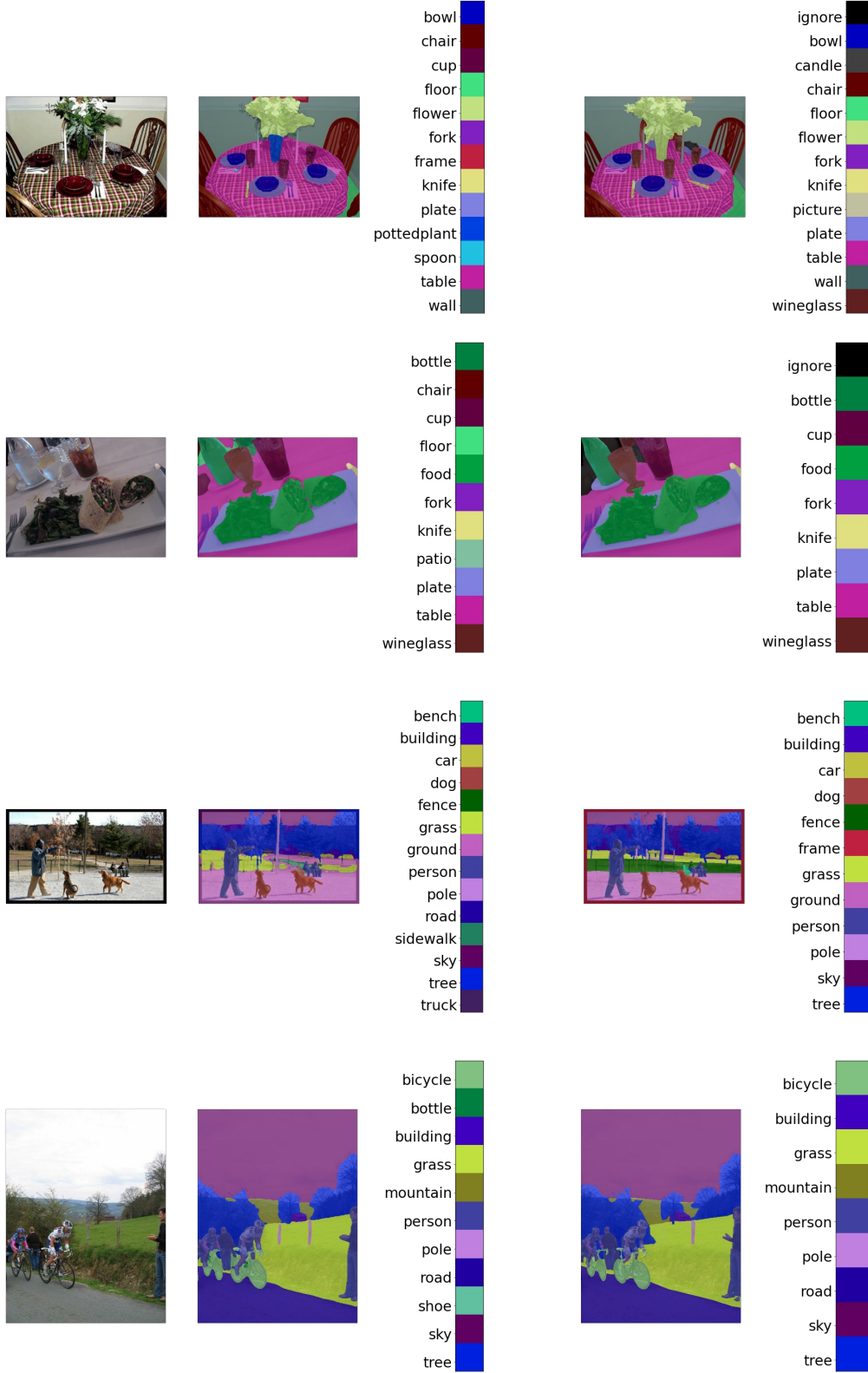


Figure 11: **Qualitative results of DaTaSeg directly transferring to PASCAL Context semantic dataset with 459 categories (PC-459).** The results demonstrate DaTaSeg has good generalization ability, and enables open-vocabulary segmentation. For each row, the left is the input image, the middle is our prediction, and the right is groundtruth. With a ViTDet-L backbone.

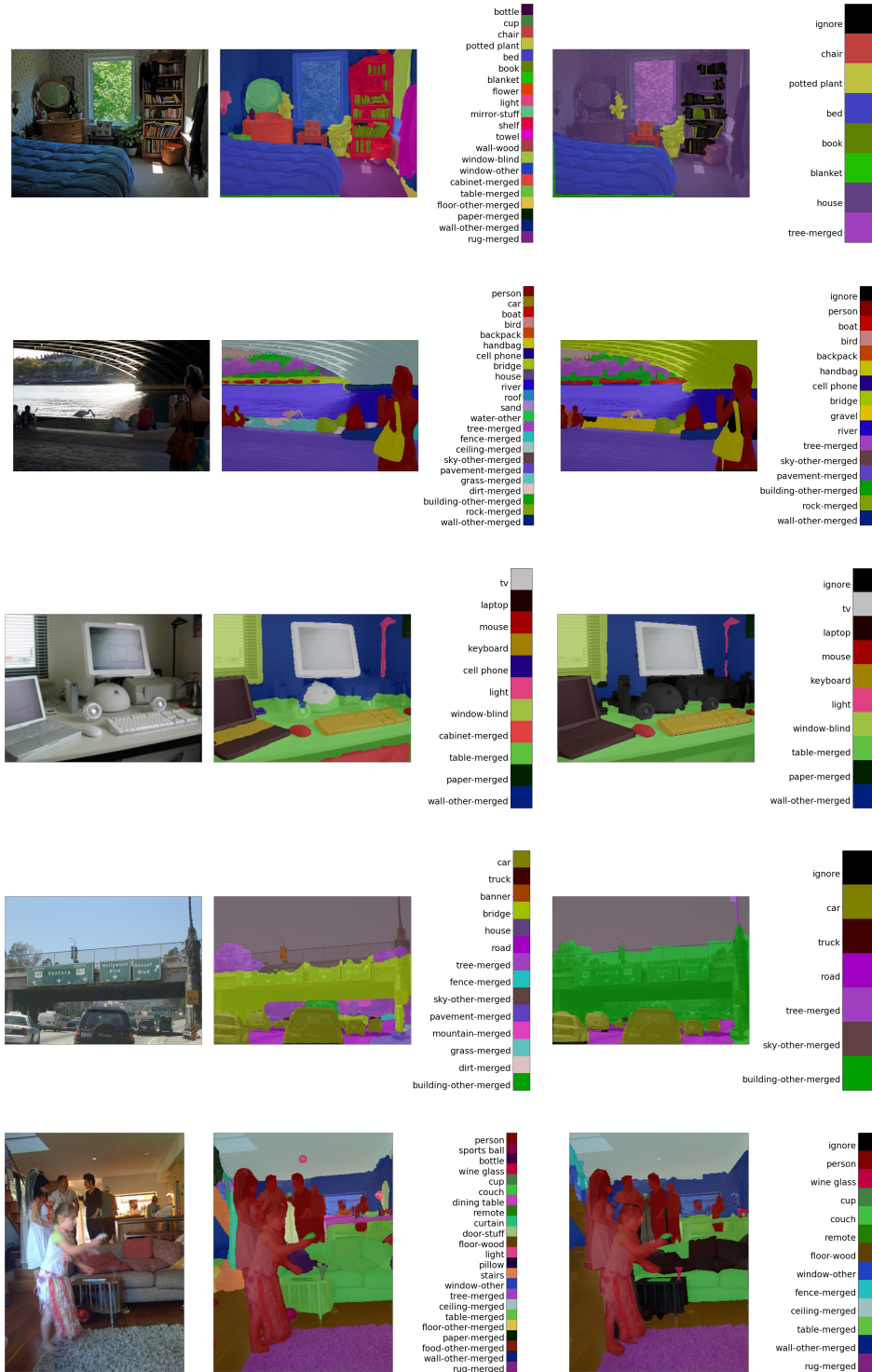


Figure 12: **Qualitative results on COCO semantic dataset.** DaTaSeg does high-quality semantic segmentation on COCO. Note that DaTaSeg trains on COCO panoptic. For each row, the left is the input image, the middle is our prediction, and the right is groundtruth. Our model is with a ViTDet-L backbone.

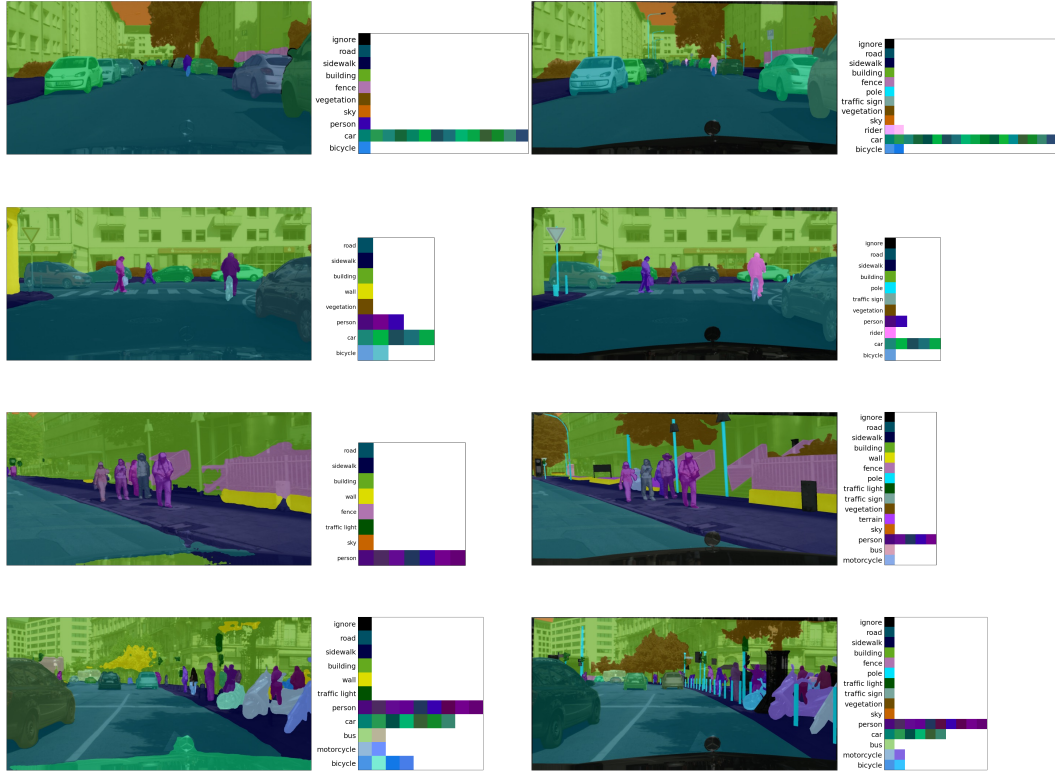


Figure 13: **Qualitative results of DaTaSeg directly transferring to Cityscapes panoptic dataset.** Cityscapes focuses on street view, which is different from all training datasets. The results demonstrate good generalization ability. For each row, the left is our prediction and the right is groundtruth. Our model is with a ViTDet-L backbone.